

# An Effective Analysis of Macular edema Severity for Diabetic Retinopathy

M.Ramya<sup>#1</sup>, S.Vijayprasath<sup>#2</sup>

<sup>#1</sup>M.E Communication systems, M.Kumarasamy college of Engineering, Karur, Tamilnadu, India

<sup>#2</sup>Department of ECE, M.Kumarasamy college of Engineering, Karur, Tamilnadu, India

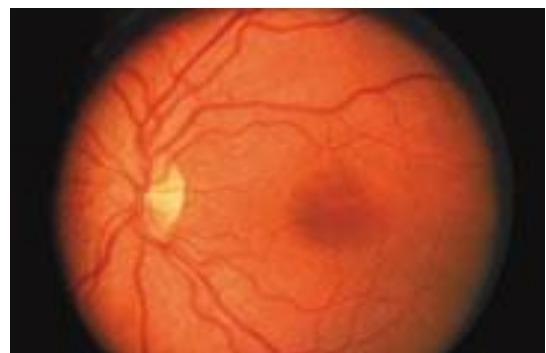
**ABSTRACT**— Recently, we have many researches on the fundus image for the detection of abnormality. Diabetic retinopathy (DR) is the damage of retina caused by complication of diabetes which results complete vision loss. Macula is responsible for our pinpoint vision. Diabetic macular edema (DME) is the major problem for the diabetic patients. Several techniques have been reported about an automated solution for the diabetic macular edema detection. An automated system for early detection of macular edema should classify all possible exudates present on the surface of retina. In this paper, two simple single class classifiers are used for the detection of abnormality. The normal retinal images are trained in these classifiers for the classification. The performance of the proposed methodology with the existing systems is evaluated based on classification accuracy. By finding the exudate, the proposed PCA DD classifier yields the highest classification accuracy compare to the Gaussian DD classifier. The overall severity accuracy for Gaussian DD and PCA DD is 84% and 92% respectively. Experimental result shows the superior nature of PCA classifier in terms of performance measures.

**KEYWORDS**— Diabetic macular edema, Diabetic Retinopathy, Fundus, Hard exudates, retina

## I. INTRODUCTION

Retinopathy is the group of noninflammatory eye disease. Diabetic retinopathy (DR) is a disorder of the eyes which occurs in patients having diabetes. Early detection and treatment is essential to prevent the DR from its severe stage. Hypoalbuminemia is often found in diabetic patients, as a major retinal disease and subsequent loss of protein in the proteinuria. The decreased plasma protein concentration decreases the intravascular oncotic

pressure. This in turn results in net fluid movement into the retinal tissues. The person who has diabetics with longer year there is a chances of developing diabetic retinopathy. This systemic disease can degenerate DME and their treatment and control can help to resolve DME. The patients with retinopathy on premature stage, have no symptoms, but at the mature stage, symptoms such as cloudy vision or blind spots may develop in [1]-[3].



(a)



(b)

Fig. 1 (a) A Normal retina, (b) A retina showing signs of Diabetic Retinopathy.

Eventually it will develop blindness if it is untreated. Complete eye exam is the only way to know whether the person have diabetic retinopathy or not. The diabetic patients should examine their eye every year once. If the DR is found special treatments can prevent future vision loss. Macula is found at the centre of the retina where the incoming rays of lights are focused. The macula is very important and it is responsible for what we see straight in front of us, the vision needed for full activities and for our ability to see colour. Macular edema is often complication of diabetic retinopathy. The fluid and protein deposits collect on or under the macula of the eye, cause it to thicken the macula portion. Fig. 1 differentiates the normal retinal image and abnormal retinal image by showing signs of diabetic retinopathy in the fundus system. The symptom of DME was based on the HE location with respect to the macula region.

Hard exudates have been used to grade the risk of macular edema. In the retina, the yellow spots near the macula are called hard exudates. The substances like lipid break-down from the blood vessels. This leads to blur or dim the viewing power of an eye. Subsequently the severity risk also classified for that DME detection. The risk for DME increases when the HE locations move toward the macula and the risk will be higher when they were within the macula. Usually Diabetic macular edema (DME) can be evaluated directly or indirectly. The manual examination (direct) is by using Stereoscopy or optical computed tomography images [6]. And in the other way of indirect examination is done by the presence of hard exudates in the retina. This indirect way is taken into an account for the automatic assessment of the disease and the severity level measurement in [7], [8], and [9]. For the detection of exudate the optic disk boundary detection reduce the workload. A deformable model guided by regional statistics was used to detect the optic disk boundary. The use of regional information gives robustness against intensity variations that rise due to vessels [22].

The remainder part of this paper prepared as follows. The section II gives the Literature review for the abnormality detection. In section III, gives the brief explanation with different algorithms and classifiers for the processing steps. Finally, the paper is concluded in section IV.

## II. BACKGROUND

Many techniques have been proposed for the detection of abnormality in colour fundus images. The datasets are publicly available with high contrast compressed (jpeg) images [25]. The images from these datasets are taken for the evaluation purpose. Different filters and classifiers have been used for the automatic detection of exudates. These techniques help the doctor to diagnose the disease as earlier as possible.

*Silberman et al. [1]* briefly discuss about a case for automatic detection of diabetic retinopathy. An automated system helps local health workers to detect seriousness of diabetic retinopathy cases without the need for local ophthalmology experts. In addition it also discuss about

the potential force on early detection of DR. In the retinal images there are four specific indicators namely micro aneurysms, exudates, hemorrhages, cotton wool spots. Among these, the primary focuses on about the detection of exudates. For the preprocessing the global colour-balancing operation is performed. For the SIFT feature extraction the segmentation mask is created during preprocessing because the optic disk and the exudates have the same intensity. They mask the optic disk and subsequently mask the non-retinal background component in the feature extraction. Finally the images were trained using 2000 negative and 1309 positive patches by the Gaussian SVM classifier [10]. The classification score is greater than 93%. From the SIFT feature extraction of 1000 images, the SVM classifier detect that 87 images having exudates.

*Hatanaka et al. [2]* determine the both Hemorrhages and exudate in ocular images. The detection of the Hemorrhages and the exudates is done by the length-to-width ratio analysis. It avoids the fluorescein angiograms. In the detection process the blood vessels were eliminated by examining the structure of blood vessels. In this, the vessels in the centrelines are extracted and eliminated to avoid the incorrectly detected vessels. Finally, the funicular shapes were eliminated to enhance the detection of hemorrhage. By evaluating the length-to-width ratio [11], the remaining false positives are eliminated accurately. Normally the ratio value was small when the candidate is incorrectly detected as vessels. The detection of exudates is same as the hemorrhage detection. Since the exudates are segmented by thresholding technique. The only difference is that the false positives are eliminated by the contrast. For 109 fundus images, the detection of exudates results with a sensitivity of 77% when the specificity was 83%.

*Osareh et al. [3]* combines the computational intelligence and pattern recognition with machine learning techniques to analyze the diabetic retinopathy. Two steps have been performed for the pre-processing. In the first step, the colour retinal images are normalized by using histogram specification [12]. In the second step the local contrast enhancement is performed to increase the contrast level of exudates in [13]. The segmentation of retinal image is done by using two-stage colour segmentation algorithm based on Gaussian-smoothed histogram analysis and FCMs clustering [14]. After segmentation the feature is extracted by using Gabor filters based on iris recognition. For selecting the best subset from the input images, the genetic-based algorithm (GA) is used for the result of better classification. The Neural network classifier classifies the segmented regions [15]. Over 150 images this scheme achieves sensitivity of 96% and specificity of 94.6%. For finding the HE, the background suppression approach was introduced by using the technique background estimation, including median filtering, morphological operations and clustering. These approaches are sensitive to illumination changes due to

imaging conditions.

Li et al. [4] make use of the prior knowledge of the retinal images. For the detection purpose first the optic disk is localized by PCA which make use of the top-down strategy for extract the common characteristics among the training images. Boundary of the optic disk is detected by Modified ASM. It consists of building a point distribution model (PDM) from training set in [16]. Then the fovea is estimated at the centre of candidate region. A polar coordinate system centred on the fovea is selected in this work. The radii of the three fovea-centred circles from the innermost to the outermost correspond to (1/3) DD, 1DD and 2DD respectively. Finally the exudates are detected by region growing [17]. In this the retinal image is subdivided into 64 subimages. Exudate detection is performed in each subimage. The resultant sensitivity and specificity is 100% and 71% respectively. The proposed algorithm were failed because a large area of lesions around the optic disk in some images and there is no such case in the training set. Model based approach is quite complicate while compare to other.

Giancardo et al. [5] introduced two methods for the detection of exudates. In this it avoids the ground-truthed lesion training sets because it is critical to obtain, prone to human error and it is a time consuming process. In preprocessing background estimation is done by median filter. Finally the dark structures and bright structures were differentiated by this histogram. For the detection of exudates, they have implemented two techniques by assigning the score for each exudate candidate. The external edges of the lesion are tried to capture by the kirsch's edges [18]. This edge detector is based on the kernel k evaluated at 8 different directions on  $I_g$ . The output is stored in the final  $I_{kirsch}$  image. The outputs are evaluated by using the threshold value  $th_{fin} \in \{0:0.5:30\}$ . In the stationary wavelets, it tries to capture the strong peaks at the centre of exudates. It can be performed up to the second level on  $I_g$ . The outputs are evaluated by using the threshold value of  $th_{fin} \in \{0: 0.05: 1\}$ . The well-defined edges of HE also been used as a hint to recognize candidate pixels. These methods require 2.4 and 1.9 seconds per image for the wavelet and kirsch's edges. Edge detection give up noisy results and hence preprocessing and post processing steps are required to decrease the large number of false candidates.

### III. PROPOSED METHOD

In the proposed work, the HE detection and severity classification is done by using Gaussian DD and PCA DD classifier. The performance of both classifiers is compared with the accuracy classification. For the clear detection some operations are performed on the images in step by step manner. Those operations are explained below with flow diagram. Here the operations are not preprocessing operation because the images were taken in the database. The database images have high resolution and high contrast. The preprocessing is taken into an account only

for enhancing the image and prior to computational processing.

It involves removing low-frequency surroundings noise, normalizing the strength of the individual unit of an image and removing reflections. The detection and severity classification steps are shown in Fig. 2. Here the flow diagram gives overall idea about our project. For both classifiers the processing steps are same up to step 5. After that the detection and severity classification is done independently. Finally the performance Parameters are evaluated for both classifier. The Parameters such as Sensitivity, Specificity, accuracy and Precision is compared. In addition the severity accuracy is calculated for the three stages of detection.

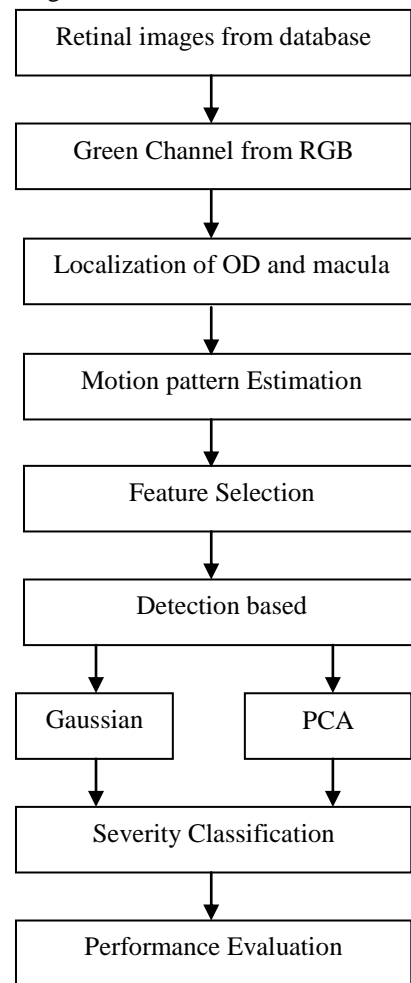


Fig. 2 Flow diagram for the detection and assessment of DME

#### A. Localization of Optic disk and Macular region

The images in the database are in the form of RGB colour combination. First the green channel is selected from the RGB component. The selection of green channel as

$$g = \frac{G}{R+G+B} \quad (1)$$

The green channel interest denoted as  $I$  gives a clear contrast and high intensity compared to Red and Blue colour component. The green channel interest  $I$  forms the input for all upcoming processing. Next the Optic disk and macular region were detected by the intensity variation in the pixels. The optic disc is noticeable and brightest region, where the macular region is the darkest region in the fundus image. The macula is the central region of the given input image. Their centroids are detected using [19] and superimpose those centroid locations on the input image. The large and bright region is located as optic disc that consist of pixels with the highest gray levels in [20] and [21]. In the fundus image the large lesions are similar to optic disc lead to false detection. The optic disc is detected and masked using [22]. Subsequently the macular region also masked same as optic disc. Both the optic disc and macular region is detected by creating bounding box on that particular region. The detection and masking is shown in Fig 3.

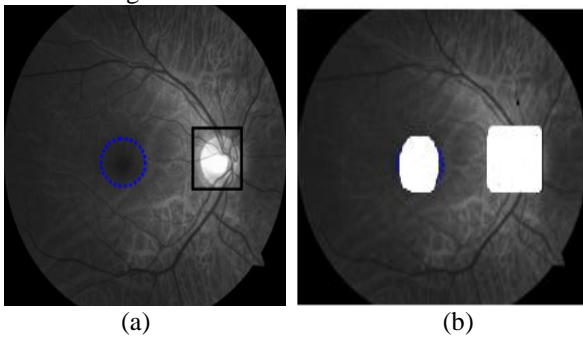


Fig. 3 Result of macula and OD detection (a) Detection of OD and macula (b) Mask of OD in rectangle and macula in circle.

### B. Motion Pattern Estimation

Motion estimation is the process of determining motion vectors that describe the transformation from one 2D image to another image. The given image is transformed to an intermediate representation called motion pattern that spatially look up the HE presence regardless of their size. This is followed by foundation of global features on motion pattern for detection of HE. The images are rotated by angle degrees in a counterclockwise direction around its center point to induce the motion pattern. The rotation step is  $-1^\circ$  and maximum angle is  $-90^\circ$ . Motion pattern  $I_{MP}$  is obtained by using the union operation as the coalescing function  $f$  [9]. Let the given input image  $I$  is denoted as  $I(\vec{r})$ . A motion pattern  $I_{MP}$  for  $I$  is derived as follows:

$$I_{MP}(\vec{r}) = f(G_N(I(\vec{r}))) \quad (2)$$

Where vector  $r$  denotes the pixel location.  $G_N$  is a transformation representing the induced motion. Motion pattern detect a change in position of an object. Let  $N$  be the transformed images generated by  $G_N$  combined using  $f$  to coalesce the sampled intensities at each pixel location in (2).  $G_N(I)$  is expressed as follows:

$$G_N(I) = \{R_{\theta_n}(I)\} \quad (3)$$

Where  $R$  is the rotation matrix. The rotation angle  $\theta_n = n\theta_0$  with  $n=0,1,\dots,N$ ;  $\theta_0$  denotes the rotation step. Since the severity of risk is measured by the radial distance of HE in the circular image [9]. For the discriminability between normal and abnormal retinal image the mean and maximum were consider in this work [9]. These are defined as follows:

$$I_{MP}^{mean}(\vec{r}) = \frac{1}{N} \sum_{n=0}^{N-1} R_{\theta_n}(I(\vec{r})) \quad (4)$$

$$I_{MP}^{max} = \max_{n=\{0,\dots,(N-1)\}} R_{\theta_n}(I(\vec{r})) \quad (5)$$

From the two equations the mean tries to achieve the averaging effect observed in motion blur and the maximum tries to exploit the fact that HE usually appear brighter than any other structures in the background at the same radial distance. Here the Shannon's entropy is calculated for the motion pattern  $I_{MP}$  is defined as  $H(Y)$  at every point  $Y$  in the magnitude of image  $\nabla I_{MP}$ . The entropy is computed over a local neighborhoods  $\Omega$  of  $Y$  to create an entropy map. The total entropy is computed by summing the entropy at every point  $Y$  as follows:

$$H_{MP} = \sum_Y H(\nabla I_{MP}(Y)) \quad (6)$$

The discriminability  $d$  of normal and abnormal retinal images is the difference between the entropy values for normal and abnormal images

$$d = |H_{MP}^{abnormal} - H_{MP}^{normal}| \quad (7)$$

### C. Feature Selection

In model construction, feature selection is the process of selecting a subset of relevant features. Feature selection is also useful as part of data analysis process, it shows which features are important for prediction, and how these features are related. It provides the benefits when constructing analytical models such as improved model interpretability, lower training times, and enhanced generalization by reducing overfitting. Motion pattern is well defined by using descriptor derived from the Radon space. The radon transform method is used for the feature selection in [9]. This provides the rotation pattern for the mean values of the given image. Then these mean vectors are passed to the radon transform method to extract the rotation pattern estimation and in the next step we extract the feature values of the image.

The radon function computes the line integrals from multiple sources along parallel paths in a certain direction. A projection of a two-dimensional function  $f(x, y)$  is a set of line integrals. The beams are spaced 1 pixel unit apart. To represent an image, the radon function takes multiple parallel-beam projections of the image from different angles by rotating the source around the center of the

image. Since the transformation transform two dimensional images with lines into a domain of possible line parameters, where each line in the image will give a peak positioned at the corresponding line parameters. The radon transform of  $f(x, y)$  is computed as

$$P_{\alpha}(r) = \int_{-\infty}^{+\infty} \int_{-\infty}^{+\infty} f(x, y) \delta(r - x \cos \alpha - y \sin \alpha) dx dy \quad (8)$$

Where  $r$  is the Perpendicular distance from a line to the origin and  $\alpha$  is the angle formed by the distance vector. First a vector response for every angle  $\alpha$  is obtained by projecting the image  $I_{MP}$  and then concatenates the responses  $P_{\alpha}$  for different orientations to derive the desired feature vector. The motion pattern  $I_{MP}$  enhances the spatial extent of any HE that may be present. Due to the intensity variation of HE the normal retina feature vector have uniform values and the abnormal retina feature vector have several peaks in its profile. Thus the feature vectors are used for learning the subspace corresponding to normal images.

#### D. Detection of Macular edema

By learning normal cases, the detection of macular edema is achieved using two types of classification. A classification boundary is formed in the feature space around the subspace corresponding to normal cases. Then the new image is projected to this feature space for the classification. If that new image is lies within this boundary, then it is classified as normal otherwise it is abnormal. For the abnormality detection two single class classifiers are used in this classification work: Gaussian data description and Principle component analysis data description (PCA DD).

1) *Gaussian DD*: By using Gaussian distribution, the normal class is modeled in an image. The mean  $\mu$  and covariance  $\Sigma$  are calculated for the normal training set. Then for the new image classification, the Mahalanobis distance is measured between the new image and normal subspace. Mahalanobis distance is used to find outliers of multivariate data. In a scatter plot of multivariate data, the origin will be at the centroid of the points (the point of their averages). It is also used to measure nearness and farness in terms of the scale of data. For the new case of classification, the Mahalanobis distance is computed as

$$D(g(I_{MP})) = (g(I_{MP}) - \mu)^T \Sigma^{-1} (g(I_{MP}) - \mu) \quad (9)$$

2) *PCA DD*: In the PCD DD the linear subspace is defined for the normal images. The subspace is described by the Eigen values corresponding to the covariance matrix  $\Sigma$  of the training set. The new case is again reconstructed as  $g(I_{MP})_{proj}$  by projecting that new case to the subspace. Based on the reconstruction error the new image is classified to be normal. The feature vectors

$g(I_{MP})$  were projected on to six dimensions to compute the reconstruction error. For the classification, the reconstruction error is computed as

$$e(g(I_{MP})) = \|(g(I_{MP}) - g(I_{MP})_{proj})\|^2 \quad (10)$$

In both data description the classification between normal and abnormal images, the threshold ranging from 0 to 1 was applied on the parameter  $D(g(I_{MP}))$  and  $e(g(I_{MP}))$ .

#### E. Severity of Macular edema

Considering 1 optic disk diameter from the center, is the key interest to detect the risk of severity. The classification is divided into three types of cases. Those are normal case, moderate case and severe case. If there is no HE present in the fundus image, that image is classified as normal image otherwise it is classified as affected image. The location of HE is not inside macula, hence it is stated as a moderate case. On the other hand the HE is within the macula, hence the case is deemed severe. In the normal fundus image, the macula is darker than other regions and it is characterized by rotational symmetry. A symmetry measure  $S$  is defined as the second norm of the distance between the histograms of diametrically opposite pair of patches ( $P(\theta_i)$  and  $P(\theta_i + \pi)$ ). In the circular database images eight patches ( $P_i$ ) were created by using eight angular samples. A histogram of 10 bins was computed for every patch. Here only the last five bins are used for measuring the symmetry because in the histogram, the intensities corresponding to HE contribute mostly to the higher bins and the preprocessing step was performed to eliminate any intensity bias as in [24]. For DME moderate or severe risk the degree of abnormality is assessed by using a threshold on the symmetry measure  $S$ . Let  $S_{max}$  and  $S_{min}$  be the maximum and minimum symmetry values for normal images. Then the abnormal image  $I_a$  is determined by comparing the symmetry measure of this image  $S(I_a)$  against a threshold  $T$  as follows:

$$\text{Severity}(I_a) = \begin{cases} \text{moderate}, & \text{if } S(I_a) \leq T \\ \text{severe}, & \text{otherwise} \end{cases}$$

To be a percentage  $p$  of the maximum symmetry value for normal images, the threshold value is selected as

$$T = p(S_{max} - S_{min}) + S_{min}.$$

For  $T$  permits the value of  $p$  to be in [0-1]. To achieve highest classification accuracy for the severe class of DME images, it is desirable to select a low value for  $p$ .

### IV. RESULT AND PERFORMANCE ANALYSIS

The experiments for assessing the proposed method were performed on publicly available MESSIDOR [25] database of colour fundus images. In this part the

experimental results are compared between Gaussian DD and PCA DD.

A. Retinal Images from Database

The image database is a collection of images. The databases are publicly available with high contrast compressed (jpeg) images [25]. The images from these databases are taken for the evaluation purpose. For the assessment of macular edema the training and testing is performed on the MESSIDOR database. MESSIDOR database consists of retinal images which has macula as a centered on that fundus images. MESSIDOR database were acquired by 3 ophthalmologic departments from Paris using a colour video 3CCD camera on a Topcon TRC NW6 non-mydratic retinograph with a 45 degree field of view. The images were captured using 8 bits per colour plane at 1440\*960, 2240\*1488 or 2304\*1536 pixels. 200 images were taken for validation of the proposed method. Over 200 images 118 images are normal and 82 images are abnormal. The severity of macular edema is based on the HE location with respect to macular region. In 82 images, 44 images are moderate case and 38 images are severe case.

B. Detection Results

Normalized threshold ranging from 0 to 1 was applied on the parameter  $D(g(I_{MP}))$  and  $e(g(I_{MP}))$  to generate receiver operating characteristic (ROC) curves for both classifiers. For the detection of macular edema and severity classification the performance comparison parameters are as follows: Sensitivity, Specificity, Precision, and Accuracy. All the parameters are calculated by using confusion matrix. It contains information about actual and predicted classifications done by a classification system. Performance of such systems is commonly evaluated using the data in the matrix. The following Table I shows the confusion matrix for a two class classifier. The entries in the confusion matrix have the following meaning in the context of our study: *TP* is defined as sick people correctly diagnosed as sick and *FP* is defined as Healthy people incorrectly identified as sick. Then *TN* is defined as Healthy people correctly identified as healthy and *FN* is defined as Sick people incorrectly identified as healthy.

TABLE I  
CONFUSION MATRIX FOR TWO CLASS CLASSIFIER

		Condition (as determined by "Gold Standard")	
		Condition Positive	Condition Negative
Test outcome	Test outcome positive	True positive (TP)	False positive (FP)
	Test outcome Negative	False negative (FN)	True negative (TN)

Sensitivity measures the proportion of actual positives

which are correctly identified as such that is the proportion of a positive test, given that the patient is ill. This can be written as  $Sensitivity = TP/(TP+FN)$ . Then Specificity measures the proportion of negatives which are correctly identified as such that is the proportion of negative test, that the patient is well. It can also be written as,  $Specificity = TN/(TN+FP)$ . The Precision is the proportion of the predicted positive cases that were correct, as calculated using the equation:  $TP/(TP+FP)$ . Finally, the Accuracy is the proportion of the total number of predictions that were correct. It is determined using the equation:  $Accuracy(AC) = (TP+TN)/(TP+FP+FN+TN)$ .

C. ROC Plots

The detection trade-off can be represented graphically as a receiver operating characteristic (ROC) curve. Fig. 4 and Fig. 5 depict the ROC curves for MESSIDOR database using Gaussian DD and PCA DD classifiers respectively. The plot indicates that the performance of both classifier and give better performance of PCA classifier than Gaussian classifier.

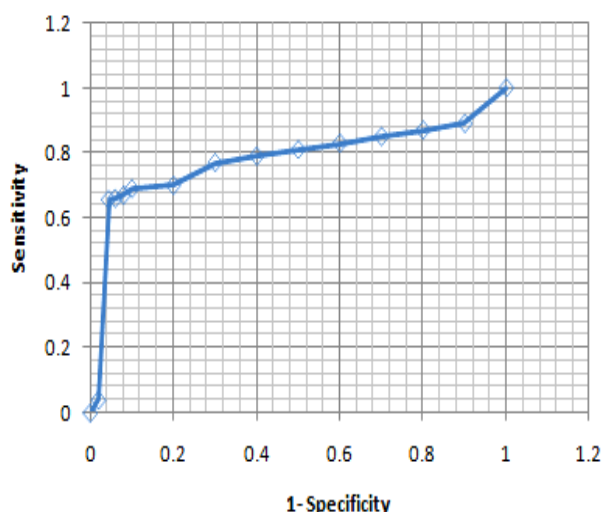


Fig. 4 ROC curve for Gaussian—MESSIDOR

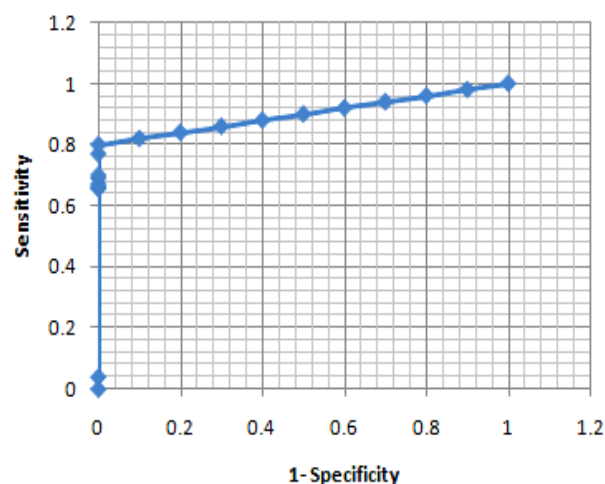


Fig. 5 ROC curve for PCA—MESSIDOR

In Table II shows the calculation result for the performance parameter. An aggregate performance of 86% specificity with 88% sensitivity is observed for Gaussian DD. For the PCA DD classification 92% specificity with 100% sensitivity is observed. Then the accuracy for the detection is 86% and 94% for Gaussian DD and PCA DD respectively. The best performance is achieved for a rotation step of 1 degree with PCA DD classification. Table III shows the severity classification for all three type of cases. Here the threshold value is in percentage ( $p$ ) as 10% for the S value for normals and for the moderate case 30%. The Overall Accuracy for Gaussian DD is 84% and 92% for PCA DD.

TABLE II  
PERFORMANCE CLASSIFICATION FOR NORMAL AND ABNORMAL CASES IN MESSIDOR DATABASE

Parameters	Gaussian DD	PCA DD
Sensitivity(%)	88	100
Specificity(%)	86	92
Precision(%)	66	80
Accuracy(%)	86	94

TABLE III  
SEVERITY CLASSIFICATION—MESSIDOR

Parameters	Gaussian DD	PCA DD
Overall Accuracy(%)	84	92
Normal Accuracy(%)	84.74	89.83
Moderate Accuracy(%)	78.94	94.73
Severe Accuracy(%)	86.36	95.45

### V. CONCLUSIONS

In this paper, we examine towards the development of an existing automated methods for the detection and severity classification of diabetic retinopathy. Diabetic retinopathy is the new cause of blindness at the age from 20 to 74. The macular edema disease affects 10 percentages of all patients who had diabetics for 10 years or more. This paper also describes the automatic assessment technique for the diabetic retinopathy with new method, which helps the diabetics to diagnosis the disease at the early stage for the prevention from vision loss [23]. The proposed method reduces the effort of building CAD scheme by removing the need for annotated abnormal images. In contrast [24], removal of blood vessels is not required. Moreover there is no need for either preprocessing the original images or post processing the results, to handle the false alarms. By using this motion pattern generation and radon transformation we can apply for the abnormal indicators such as microaneurysms, hemorrhages, and cotton wool

spots for the better performance.

### REFERENCES

- [1] R. F. N. Silberman, K. Ahlrich, and L. Subramanian, "Case for automated detection of diabetic retinopathy," Proc. AAAI Artif. Intell. Development (AI-D'10), pp. 85–90, Mar. 2010.
- [2] Y.Hatanaka, T. Nakagawa, Y. Hayashi, Y. Mizukusa, A. Fujita, M.Kakogawa, K. K.M. D. , T. Hara, and H. Fujita, "Cad scheme to detect hemorrhages and exudates in ocular fundus images," in Proc. SPIE Med. Imag. 2007: Comput.-Aided Diagn., Mar. 2007, vol. 6514, pp. 2M1–2M8.
- [3] A.Osareh, B. Shadgar, and R. Markham, "A computational-intelli-gence-based approach for detection of exudates in diabetic retinopathy images," IEEE Trans. Inf. Technol. Biomed., vol. 13, no. 4, pp. 535–545, Jul. 2009.
- [4] H. Li and O. Chutatape, "A model-based approach for automated feature extraction in fundus images," in Proc. 9th IEEE Int. Conf. Comput. Vis., Oct. 2003, vol. 1, pp. 394–399.
- [5] L. Giancardo, F. Meriaudeau, T. P. Karnowski, Y. Li, K. W. Tobin, Jr., and E. Chaum, "Automatic retina exudates segmentation without a manually labelled training set," in Proc. 2011 IEEE Int. Symp. Biomed. Imag: From Nano to Macro, Mar. 2011, pp. 1396–1400.
- [6] M. R. Hee, C. A. Puliafito, C. Wong, J. S. Duker, E. Reichel, B. Rutledge, J. S. Schuman, E. A. Swanson, and J. G. Fujimoto, "Quantitative assessment of macular edema with optical coherence tomography," Arch. Ophthalmol., vol. 113, no. 8, pp. 1019–1029, Aug. 1995.
- [7] C. P. Wilkinson, F. L. Ferris, R. E. Klein, P. P. Lee, C. D. Agardh, M. Davis, D. Dills, A. Kampik, R. Pararajasegaram, and J. T. Verdaguer, "Proposed international clinical diabetic retinopathy and diabetic macular edema disease severity scales," Am. Acad. Ophthalmol., vol. 110, no. 9, pp. 1677–1682, Sep. 2003.
- [8] NIH. 2009. Facts about diabetic retinopathy disease <http://www.nei.nih.gov/health/diabetic/retinopathy.asp>
- [9] K. Sai Deepak and Jayanthi Sivasamy, "Automatic Assessment of Macular Edema From Color Retinal Images," IEEE Transactions on Biomedical Engineering, vol. 31, no. 3, pp. 766-776, Mar 2012.
- [10] Zhang, X., and Chutatape, O. 2005. Top-down and bottom-up strategies in lesion detection of background diabetic retinopathy. In CVPR '05: Proceedings of the 2005 IEEE Computer Society Conference on Computer Vision and Pattern Recognition (CVPR'05) - Volume 2, 422–428. Washington, DC, USA: IEEE Computer Society.
- [11] O. R. Mitchell, C. R. Myers and W. Boyne, "A max–min measure for image texture analysis," IEEE Transactions on Computers, C-2 (4), 408–414, 1977.
- [12] R. Gonzalez and R. Woods, Digital Image Processing. Reading, MA: Addison-Wesley, 1992.
- [13] C. Sinthanayothin, "Image analysis for automatic diagnosis of diabetic Retinopathy," Ph.D. dissertation, King's College of London, London,U.K., 1999.
- [14] Y. Lim and S. Lee, "On the color image segmentation algorithm based on the thresholding and the fuzzy c-means techniques," Pattern Recogn., vol. 23, no. 9, pp. 935–952, 1990.
- [15] C. Bishop, Neural Networks for Pattern Recognition. London, U.K.: Oxford Univ. Press, 1995.
- [16] L. Vincent, "Morphological grayscale reconstruction in image analysis: applications and efficient algorithms," IEEE Journal of Image Processing, vol. 2, no. 2, pp. 176–201, 1993.
- [17] R A Kirsch, "Computer determination of the constituent structure of biological images,," Computers and Biomedical Research, vol. 4, no. 3, pp. 315–328, Jun 1971.
- [18] T. F. Cootes, C. J. Taylor, D. H. Cooper, and J. Graham, "Active shape models-Their training and application," Comput. Vis. Image Understanding, vol. 61, no. 1, pp. 38–59, 1995.
- [19] J. Singh, G. D. Joshi, and J. Sivaswamy, "Appearance-based object detection in colour retinal images," in Proc. Int. Conf.

- Image Process., 2008, pp. 1432–1435.
- [20] S. Tamura, Y. Okamoto, and K. Yanashima, “Zero-crossing interval correction in tracking eye-fundus blood vessels,” *Pattern Recogn.*, vol. 21, no. 3, pp. 227–233, 1988.
  - [21] Z. Liu, O. Chutatape, and S. M. Krishnan, “Automatic image analysis of fundus photograph,” *Proc. 19th Annu. Int. Conf. IEEE Engineering in Medicine and Biology Society*, vol. 2, pp. 524–525, 1997.
  - [22] G. D. Joshi, J. Sivaswamy, K. Karan, and S. R. Krishnadas, “Optic disk and cup boundary detection using regional information,” in *Proc. Int. Conf. Image Process.*, 2010, pp. 948–951.
  - [23] J. Davidson, T. Ciulla, J. McGill, K. Kles, and P. Anderson, “How the diabetic eye loses vision,” *Endocrine*, vol. 32, pp. 107–116, Nov. 2007.
  - [24] K. S. Deepak, G. D. Joshi, and J. Sivaswamy, “Content-based retrieval of retinal images for maculopathy,” in *Proc. 1st ACM Int. Health Inf. Symp.*, 2010, pp. 135–143.
  - [25] MESSIDOR, Jun. [Online], Available: <http://messidor.crihan.fr/index-en.php>.